Electronic Supplementary Material (ESI) for Physical Chemistry Chemical Physics.

Hot kinetic model as a guide to improve organic photovoltaic materials

Andrey Yu. Sosorev[1], Dmitry Yu. Godovsky[2], Dmitry Yu.Paraschuk[1,3]

1.Faculty of Physics and International Laser Center, M.V.Lomonosov Moscow State University, Moscow 119991 Russia.
2. Institute of Elementoorganic Compounds, Russian Academy of Science, Moscow, Vavilova, 28
3. Enikolopov Institute of Synthetic Polymeric Materials, Russian Academy of Science, Profsoyuznaya 70, Moscow 117393, Russia

Keywords: organic solar cells, ultimate efficiency, electron transfer, charge-transfer state, reorganization energy

Supporting Information

1. Model derivation and details

1.1. Rate constants for different processes

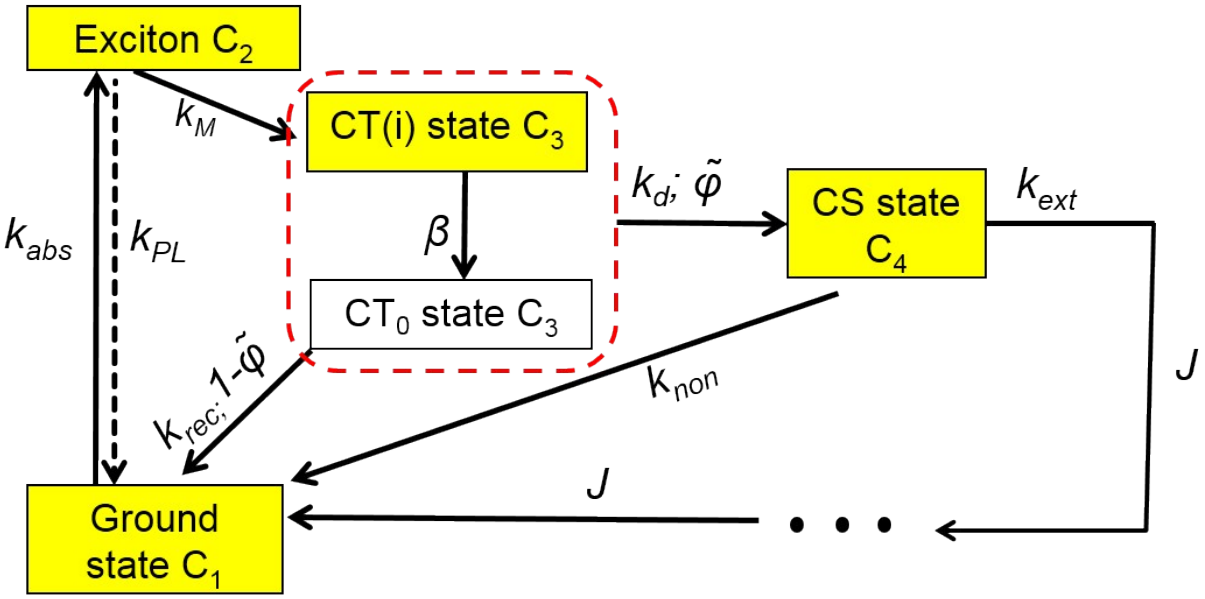

Fig. S1. Schematic of the hot kinetic model. C_i are the concentrations of charge pairs occupying these states. C_3 is the total concentration of charge pairs in all the CT states.

Fig. S1 depicts the block-scheme of the model with the considered states, electron-hole pairs' concentrations at them, and rate constants. The explicit expressions for rate constants are given below, all the rates are given per unit area.

- The photon absorption rate $k_{abs} = \Phi \cdot \alpha(E_g)$ per unit area is proportional to the photon flux Φ (assumed 10^{21} $m^{-2}s^{-1}$), the cell area S and the probability for photon absorption by the active layer $\alpha(E_g) = \frac{\int_0^\infty f(E)\varepsilon(E)dE}{\int_0^\infty \varepsilon(E)dE}$, where $f(E)$ is the spectral density of the solar spectrum, and $\varepsilon(E)$ is the absorption probability for a photon with energy E (related to the absorption spectrum of the donor).

- The photoluminescence rate is $R_{PL} = k_{PL}C_1$, where $k_{PL} = 1/\tau_0$ is the inversed PL lifetime (τ_0).
- $R_M = k_M C_1$ is the total transfer rate from the exciton state to all the CT states, where

$$k_M = \sum_i \nu_0 \exp\left(-\frac{(E_g - E_i - \lambda)}{4\lambda kT}\right), \qquad \text{(S1)}$$

In (S1), ν_0 is the attempt-to-jump frequency (assumed 10^{12} s^{-1}), λ is the reorganization energy, k is the Boltzmann constant, and T is the absolute temperature.

- Back-transfer to the exciton state is neglected.
- The geminate recombination rate is $R_{rec} = k_{rec}C_3$.
- The CT state-to-charges dissociation rate is $R_d = k_d C_3$. The corresponding rate constant is $k_d = \frac{\varphi}{1-\varphi}k_{rec}$, where φ is the probability of the CT state dissociation described by the Onsager-Braun model:

$$\varphi = \frac{1 + \frac{k_{rec}R^3}{D \cdot r_c}\frac{\sqrt{2}(-b)^{1/2}}{J\left[2\sqrt{2}(-b)^{1/2}\right]}\exp\left(\frac{r_c}{R}\right)\left(\exp\left(-\frac{r_c}{r_0}\right) - \exp\left(-\frac{r_c}{R}\right)\right)}{1 + \frac{k_{rec}R^3}{D \cdot r_c}\frac{\sqrt{2}(-b)^{1/2}}{J\left[2\sqrt{2}(-b)^{1/2}\right]}\left(\exp\left(\frac{r_c}{R}\right) - 1\right)}, \qquad \text{(S2)}$$

In Eq. (S2), D is the charges diffusion coefficient, R is the electron-hole distance at which their recombination can take place (3.5 Å in the model), r_0 is the initial separation of the electron and hole, $r_c = \frac{e^2}{4\pi\varepsilon_0\varepsilon kT}$ is the so-called Onsager radius (distance at which the electron-hole attraction energy equals kT), ε is the dielectric permittivity, and ε_0 is the electric constant. $J(x)$ is a Bessel function of order one, and $b = \frac{e^3F}{8\pi\varepsilon_0\varepsilon(kT)^2}$ is the normalized external electric field. The

diffusion coefficient D is related to the charge carrier mobility, μ: $D = \frac{\mu kT}{e}$. In the last expression, the total charge mobility is the sum of the electron and hole mobilities: $\mu = \mu_e + \mu_h$.

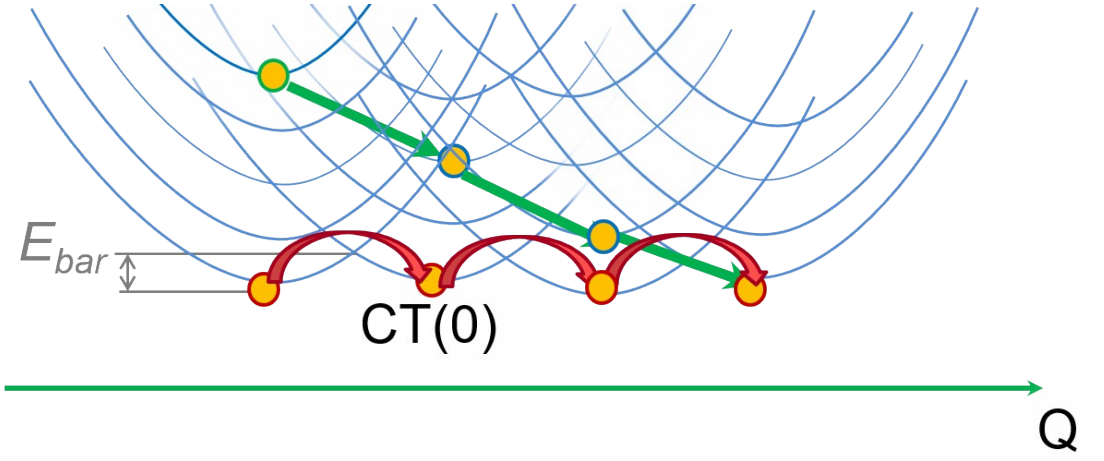

Fig. S2. Illustration of the difference in mobility of cold and hot charges. The blue parabolas depict potential curves for the states of the charged molecules. The green and red arrows depict transitions between these states. E_{bar} stands for the energy barrier that cold carriers need to overcome.

In our model, we take into account the excess energy of a hot CT state, W, by replacing the equilibrium diffusion coefficient for charge carriers by the non-equilibrium one D_{hot}: $D_{hot}(E) = \frac{\mu}{e} W$ (see Eq. (2) in the main text). The reasoning behind this assumption is that excess energy provides more pathways for transitions from this state and suppresses the role of thermal fluctuations in charge transfer. This is illustrated in Fig. S2 within the Marcus model. Enhanced mobility of the photogenerated ("hot") charges and its subsequent decrease were observed experimentally in Refs. [1-3]. Therefore, we suggest that the concept of the enhanced diffusion of hot charges is justified.

Assuming enhanced diffusion coefficients for hot charges results in changes of r_c and b as well:

$$r_{c,hot}(E) = \frac{e^2}{4\pi\varepsilon_0\varepsilon W} \quad \text{(S3)}$$

$$b_{hot}(E) = \frac{e^3 F}{8\pi\varepsilon_0\varepsilon W^2} \quad \text{(S4)}$$

In Eqs. (S5-S6), $W = E - E_{CT0}$, where E is the energy of the given CT state, and E_{CT0} is the energy of the lowest-energy CT state. The dissociation probability for the hot CT state is

$$\varphi(E) = \frac{1 + \frac{k_{rec}R^3}{D_{hot}(E)r_{c,hot}(E)} \frac{\sqrt{2}\left(-b_{hot}(E)\right)^{1/2}}{J\left[2\sqrt{2}\left(-b_{hot}(E)\right)^{1/2}\right]} \exp\left(\frac{r_{c,hot}(E)}{R}\right)\left(\exp\left(-\frac{r_{c,hot}(E)}{r_0}\right) - \exp\left(-\frac{r_{c,hot}(E)}{R}\right)\right)}{1 + \frac{k_{rec}R^3}{D_{hot}(E)r_{c,hot}(E)} \frac{\sqrt{2}\left(-b_{hot}(E)\right)^{1/2}}{J\left[2\sqrt{2}\left(-b_{hot}(E)\right)^{1/2}\right]}\left(\exp\left(\frac{r_{c,hot}(E)}{R}\right) - 1\right)} \quad \text{(S5).}$$

- For non-geminate recombination, we use the Langevin bimolecular recombination model. The recombination rate (per unit area) reads $R_{non} = k_{non} C_4{}^2 d$, where. $k_{non} = \frac{\mu e}{\varepsilon_0 \varepsilon}$.
- The charge extraction rate is $R_{ext} = k_{ext} C_4$, and the corresponding rate constant k_{ext} is determined by the electric field within the active layer, $F = (E_{HL}/e - U)/d$, and charge mobility μ: $k_{ext} = \mu F = \frac{\mu}{d}\left(\frac{E_{HL}}{e} - U\right)$
  - The photocurrent J is proportional to the charge extraction rate: $J = e \cdot R_{ext} \cdot S$, where S is the cell area

1.2. Charge thermalization: distance distribution for thermalized charges

To calculate the charge distribution after thermalization, we fix the hole at the origin and treat the "hot" electron movement as free diffusion with an non-equilibrium diffusion coefficient, D_{hot}, neglecting the electron-hole attraction. Although free electron diffusion instead of diffusion in the hole field leads to some overestimation of the charge separation probability, we consider such approximation as appropriate since the kinetic energy of the hot charge is much larger than the energy of its attraction to the hole at the initial distance. If the initial distance between the two particles was r_0, the probability density to find them at the separation distance r after thermalization time τ is assumed to be

$$w(r, r_0) = \frac{1}{N} \exp\left(-\frac{r^2}{4(D_{hot}\tau + r_0)}\right) \quad \text{(S6)}$$

where N is the normalization constant of the distribution. The total probability for the CT state dissociation to free charges is

$$\varphi_{th}(r_0) = 4\pi \int_0^\infty \varphi(r) w(r, r_0) r^2 dr, \quad \text{(S7)}$$

In Eq. (S7), $\varphi(r)$ is the probability for dissociation of a cold electron-hole pair with initial separation distance r. The $\varphi(r)$ is described by the standard Onsager-Braun model, Eq. (S2). The photocurrent is then calculated by substitution of Eq. (S7) into Eq. (4) of the main text.

2. Impacts

2.1 Optimal driving force

Fig. S3a shows power conversion efficiency as a function of the driving force ΔE for various reorganization energies λ. The curve is bell shaped with a maximum at an optimal driving force, and the value of the latter depends on λ. Specifically, the larger the reorganization energy, the lower the driving force required for efficient dissociation of the CT state. Approximately, the optimal driving force is ca. 0.2 eV larger than λ for the parameters in Fig. S3**a**; however, the difference between λ and the optimal ΔE may vary with variation of other parameters (mobility, optical bandgap, etc.). Accordingly, the optimal LUMO energy of the acceptor also depends on material parameters. The optimal acceptor LUMO E_{LUMO} as a function of E_g is shown in Fig. S3b for two λ values (the donor LUMO energy equals to E_g). For lower λ, the optimal E_{LUMO} is closer to E_g, i.e., to the donor LUMO energy, and therefore the energy loss is lower.

a)

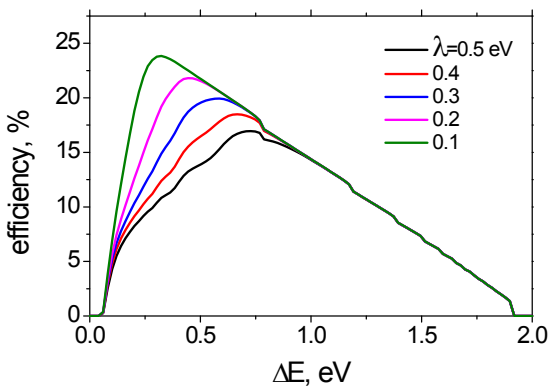

b)

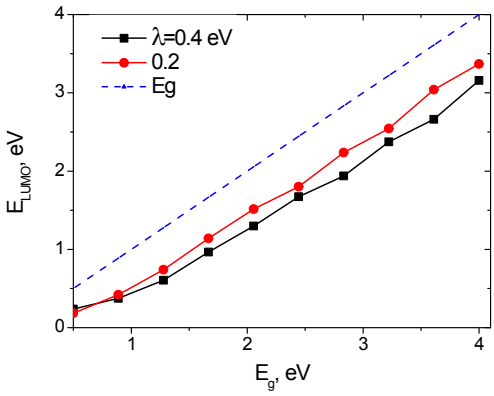

Fig. S3.(a) Power conversion efficiency as a function of the driving force for various reorganization energies. E_g=2 eV, k_{rec}=10^{10}s^{-1}. (b) Optimal acceptor LUMO energy as a function of E_g.

2.2. Impact of the recombination rate and electron-hole distance in CT state on the efficiency plot

The recombination rate is related to the lifetime of an isolated CT state τ_{rec}, i.e., that in absence of charge extraction: $k_{rec} = 1/\tau_{rec}$, and is determined by the electronic coupling between the CT state and the ground state (coupling between donor HOMO and acceptor LUMO in one-

electron picture) and the reorganization energy. In some blends, where the donor HOMO and acceptor LUMO wavefunctions strongly overlap, the isolated CT state lifetime is quite low and amounts ca. 5 ps[4]. In other blends (e.g. MEH-PPV:C60 [4]), τ_{rec}=300 ps. In state-of-the-art donor-acceptor polymer:fullerene blends, the CT state lifetime can be as long as 1200 ps[5]. It depends on the relative orientation of the molecules[6] and can be calculated using, e.g., DFT, for a given system.

Fig. S4 presents efficiency plots for different k_{rec}. The larger the k_{rec}, the stronger its influence on η, and accordingly the impact of recombination on η is diminished for low k_{rec}. Importantly, the higher the recombination rate, the larger the optimal bandgap: if recombination is fast, the charges should be more mobile, i.e. have larger excess energies to escape their parent CT states. This finding is in accordance with the results of the thermodynamic model suggested by Green in Ref. [7].

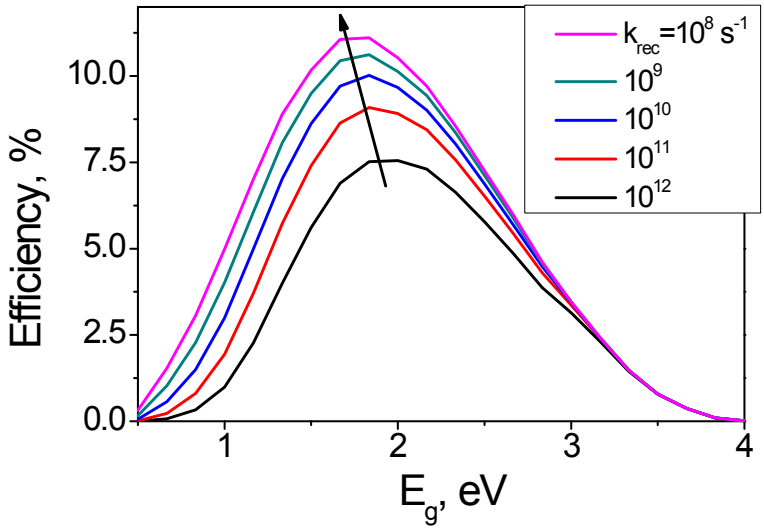

Fig. S4. Efficiency plots for different recombination rates

The model yields that the impact of r_0 on η significantly depends on the values of the other parameters. To illustrate this, we analyze two blends: "poor" one with $\gamma = \mu/k_f = 10^{-14}$ V/cm^2 (low mobility, e.g. 10^{-3} cm^2/(V·s), and/or high recombination, e. g. $k_{rec} = 10^{11}$ s^{-1}) and "good" one with $\gamma = 10^{-11}$ V/cm^2 (relatively high mobility, 0.1 cm^2/(V·s), and relatively low recombination, $\tau_{rec} = 10^{10}$ s^{-1}). Fig. S4 shows efficiency plots for the "poor" (a) and "good" (b) blends, correspondingly. For the "poor" blend, an increase in r_0 significantly improves the performance, while for the "good" blend, the efficiency is nearly not sensitive to the increase in r_0.

a) b)

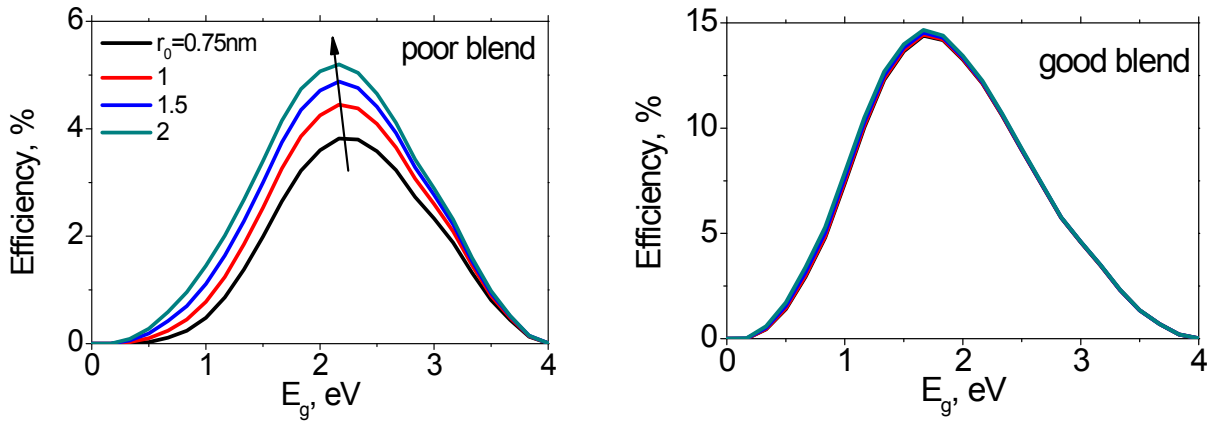

Fig. S5. Efficiency plots for various initial electron-hole separation in "poor" blend (panel a, γ=10^{-14} V/cm^2) and in "good" blend (panel b, γ=10^{-11} V/cm^2).

Some OSC materials have low charge carrier mobility (10^{-6}–10^{-4} cm^2/(V·s)) and high recombination rate of the order of $10^{10\text{-}12}$ s^{-1} [4, 8], and hence increasing the electron-hole distance in the CT state could significantly increase η. The electron-hole distance, r_0, in the CT state is determined by the distance between the centers of the electron and hole wavefunctions in the CT state and their delocalization, and can be tuned via material choice. For instance, r_0 is relatively low for polymer:polymer or homopolymer:planar acceptor (e.g. perylene diimide derivative) blends, larger for homopolymer:fullerene blends, and even larger for the blends of donor-acceptor polymers with fullerene derivatives. Therefore, the model explains the success of the OSCs based on the donor-acceptor polymers that can provide internal quantum efficiency (IQE) approaching 100% [9] and η > 10% (single junction)[10]. Donor-acceptor polymers with so-called spacers between donor and acceptor units provide a more extended CT state and show a higher charge yield[11]. When the distance between the polymer and acceptor conjugated skeletons is further increased due to bulky side chains, the charges separate more efficiently[12]. Nevertheless, the model suggests that large r_0 is unnecessary for OSC materials with high μ and low k_{rec} ("good" blends), and can hardly help to overcome the current 13% barrier in OSC efficiency.

2.3. Reduced Langevin recombination

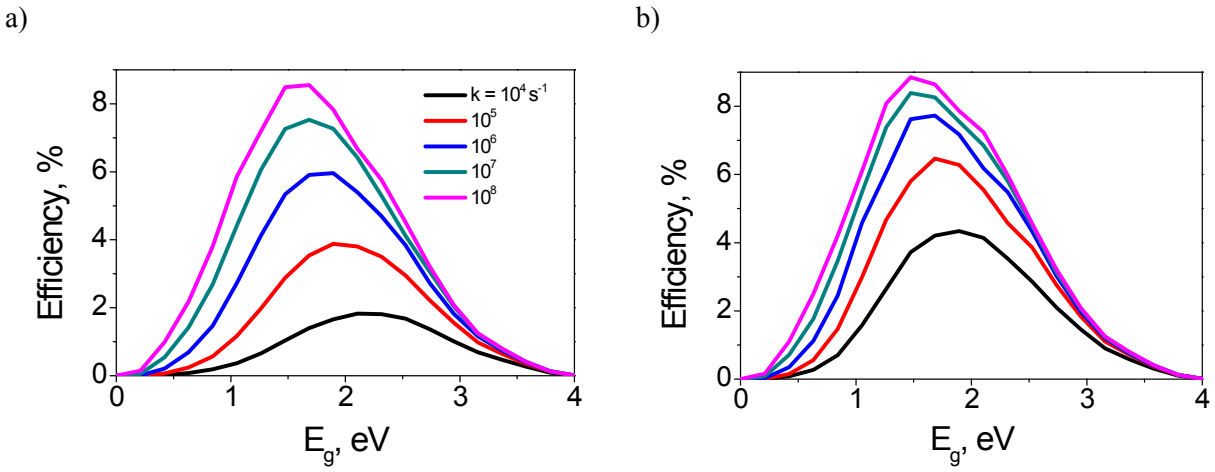

Fig. S6. Efficiency plots for different μ with Langevin recombination (a) and with 1000-fold reduced Langevin recombination (b).

The bimolecular recombination with rates up to three orders of magnitude lower than that predicted by the Langevin expression (see Section 1.1) was reported for bulk-heterojunction OSCs [13]. Reduced bimolecular recombination can increase the probability of charge separation. Fig. S6 collates the efficiency plots for different μ for Langevin recombination (a) and recombination reduced by 1000 times as compared to the Langevin one (b). For the low-efficiency blends, the reduced bimolecular recombination significantly increases the cell efficiency. However, for efficient OSCs, reducing bimolecular recombination has low impact on the cell performance.

2.4. Phase separation and other factors improving charge separation

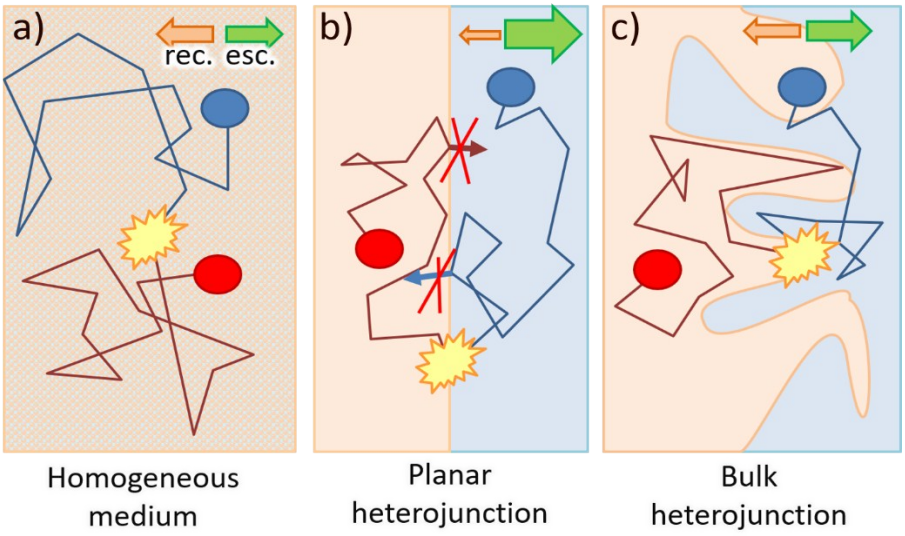

Fig. S7. CT state dissociation in homogeneous medium (a), at planar heterojunction (b) and in bulk heterojunction (c).

Fig. S7 illustrates the impact of phase separation on CT state dissociation. In homogeneous medium (a), the electron and hole motion is not restricted, in the case of planar (b) or bulk (c) heterojunction, the electron and hole motion is limited within the acceptor and donor phases, respectively. While rigorous consideration of the phase separation requires numerical modeling and is far beyond the current study, the impact of phase separation can be evaluated indirectly from the following reasoning. When one of the charges (e.g., electron) is at the interface, it can not move into the other phase, towards the opposing charge (hole), but can instead be "reflected" away from the interface, and the dissociation rate increases twice (the thicker green arrow in Fig. S7b, c). At the same time, the recombination can be provided only by the motion of the opposite charge towards the interface, and its rate decreases twice if $\mu_1=\mu_2$ (the thinner red arrow in Fig. S7b, c. Thus the dissociation-to-recombination rates ratio increases by four times:

$$\left(\frac{k_d}{k_{rec}}\right)' = \frac{2Dr_c}{k_{rec}/2\,R^3} \qquad \text{(S8)}$$

According to the derivation of the Tachiya-Onsager-Braun model[14], this means that the probability of charge separation becomes

$$\varphi(E)=\frac{1+\frac{k_{rec}R^3}{4D_{hot}(E)r_{c,hot}(E)}\frac{\sqrt{2}\left(-b_{hot}(E)\right)^{1/2}}{J\left[2\sqrt{2}\left(-b_{hot}(E)\right)^{1/2}\right]}\exp\left(\frac{r_{c,hot}(E)}{R}\right)\left(\exp\left(-\frac{r_{c,hot}(E)}{r_0}\right)-\exp\left(-\frac{r_{c,hot}(E)}{R}\right)\right)}{1+\frac{k_{rec}R^3}{4D_{hot}(E)r_{c,hot}(E)}\frac{\sqrt{2}\left(-b_{hot}(E)\right)^{1/2}}{J\left[2\sqrt{2}\left(-b_{hot}(E)\right)^{1/2}\right]}\left(\exp\left(\frac{r_{c,hot}(E)}{R}\right)-1\right)} \quad \text{(S9)}$$

Several reports suggested that favorable energy landscape can further increase the CT state dissociation probability.[15] This effect also cannot be rigorously accounted in the model, but its role can be estimated. To do this, we introduce additional parameter $\xi<1$

$$\varphi(E)=\frac{1+\frac{k_{rec}R^3}{4\xi D_{hot}(E)r_{c,hot}(E)}\frac{\sqrt{2}\left(-b_{hot}(E)\right)^{1/2}}{J\left[2\sqrt{2}\left(-b_{hot}(E)\right)^{1/2}\right]}\exp\left(\frac{r_{c,hot}(E)}{R}\right)\left(\exp\left(-\frac{r_{c,hot}(E)}{r_0}\right)-\exp\left(-\frac{r_{c,hot}(E)}{R}\right)\right)}{1+\frac{k_{rec}R^3}{4\xi D_{hot}(E)r_{c,hot}(E)}\frac{\sqrt{2}\left(-b_{hot}(E)\right)^{1/2}}{J\left[2\sqrt{2}\left(-b_{hot}(E)\right)^{1/2}\right]}\left(\exp\left(\frac{r_{c,hot}(E)}{R}\right)-1\right)} \quad \text{(S10)}$$

The role of phase separation and other abovementioned mechanisms promoting charge separation is illustrated in Fig. S8 for several blends with different material properties. Fig. S8a shows that in OSCs with low efficiency, these factors play important roles resulting in about 1.5-fold improvement of the efficiency. However, for "good" OSCs (Fig. S8b), the impact of these factors is less pronounced. The optimal E_g is not also significantly altered when they are taken into account. We therefore suggest that neglect of phase separation does not call in question our conclusions, although it underestimates the efficiencies of "poor" blends.

(a) (b)

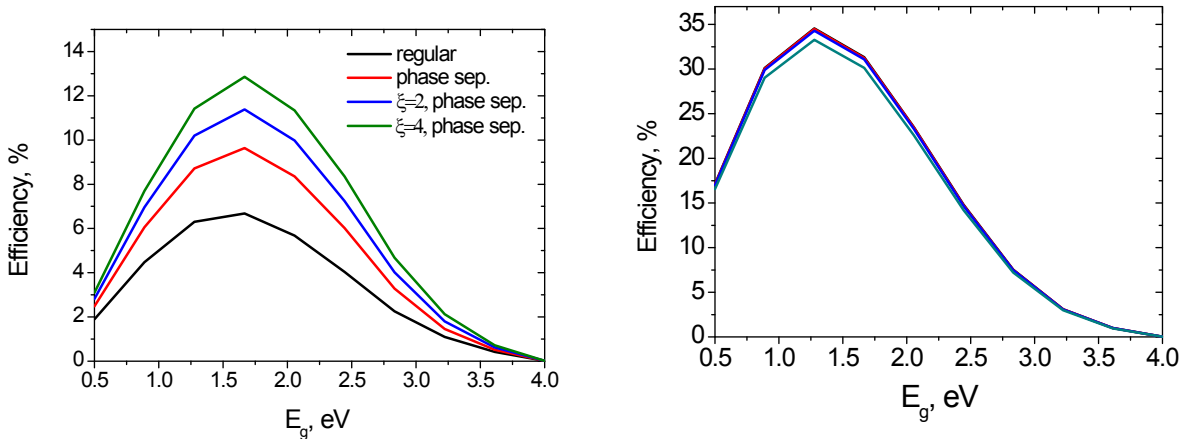

Fig. S8. Effect of phase separation on the OSC efficiency for "poor"(a) and "good"(b) blends. The parameters are: (a) μ=10^{-4} cm^2/Vs, k_{rec}=10^{11} s^{-1}, λ=0.5 eV; (b) μ=1 cm^2/Vs, k_{rec}=10^{10} s^{-1}, λ=0.1 eV.

References

1. Vithanage, D. A.; Devižis, A.; Abramavičius, V.; Infahsaeng, Y.; Abramavičius, D.; MacKenzie, R. C. I.; Keivanidis, P. E.; Yartsev, A.; Hertel, D.; Nelson, J.; Sundström, V.; Gulbinas, V., Visualizing charge separation in bulk heterojunction organic solar cells. *Nat Commun* **2013,** *4*, 2334.
2. Melianas, A.; Pranculis, V.; Devižis, A.; Gulbinas, V.; Inganäs, O.; Kemerink, M., Dispersion-Dominated Photocurrent in Polymer:Fullerene Solar Cells. *Advanced Functional Materials* **2014,** *24* (28), 4507-4514.
3. Melianas, A.; Pranculis, V.; Xia, Y. X.; Felekidis, N.; Inganas, O.; Gulbinas, V.; Kemerink, M., Photogenerated Carrier Mobility Significantly Exceeds Injected Carrier Mobility in Organic Solar Cells. *Advanced Energy Materials* **2017,** *7* (9).
4. Bakulin, A. A.; Zapunidy, S. A.; Pshenichnikov, M. S.; van Loosdrecht, P. H. M.; Paraschuk, D. Y., Efficient two-step photogeneration of long-lived charges in ground-state charge-transfer complexes of conjugated polymer doped with fullerene. *Physical Chemistry Chemical Physics* **2009,** *11* (33), 7324-7330.
5. Etzold, F.; Howard, I. A.; Forler, N.; Cho, D. M.; Meister, M.; Mangold, H.; Shu, J.; Hansen, M. R.; Müllen, K.; Laquai, F., The Effect of Solvent Additives on Morphology and Excited-State Dynamics in PCPDTBT:PCBM Photovoltaic Blends. *Journal of the American Chemical Society* **2012,** *134* (25), 10569-10583.
6. Huang, Y. S.; Westenhoff, S.; Avilov, I.; Sreearunothai, P.; Hodgkiss, J. M.; Deleener, C.; Friend, R. H.; Beljonne, D., Electronic structures of interfacial states formed at polymeric semiconductor heterojunctions. *Nature Materials* **2008,** *7* (6), 483-489.
7. Green, M. A., Radiative efficiency of state-of-the-art photovoltaic cells. *Prog. Photovoltaics* **2012,** *20* (4), 472-476.
8. Martens, H. C. F.; Huiberts, J. N.; Blom, P. W. M., Simultaneous measurement of electron and hole mobilities in polymer light-emitting diodes. *Applied Physics Letters* **2000,** *77* (12), 1852-1854.

9. Park, S. H.; Roy, A.; Beaupré, S.; Cho, S.; Coates, N.; Moon, J. S.; Moses, D.; Leclerc, M.; Lee, K.; Heeger, A. J., Bulk heterojunction solar cells with internal quantum efficiency approaching 100%. *Nature Photonics* **2009,** *3*, 297 - 302.
10. Liu, Y.; Zhao, J.; Li, Z.; Mu, C.; Ma, W.; Hu, H.; Jiang, K.; Lin, H.; Ade, H.; Yan, H., Aggregation and morphology control enables multiple cases of high-efficiency polymer solar cells. *Nat Commun* **2014,** *5*, 5293.
11. Tautz, R.; Da Como, E.; Limmer, T.; Feldmann, J.; Egelhaaf, H.-J.; von Hauff, E.; Lemaur, V.; Beljonne, D.; Yilmaz, S.; Dumsch, I.; Allard, S.; Scherf, U., Structural correlations in the generation of polaron pairs in low-bandgap polymers for photovoltaics. *Nature Commununications* **2012,** *3*, 970.
12. Holcombe, T. W.; Norton, J. E.; Rivnay, J.; Woo, C. H.; Goris, L.; Piliego, C.; Griffini, G.; Sellinger, A.; Brédas, J.-L.; Salleo, A.; Fréchet, J. M. J., Steric Control of the Donor/Acceptor Interface: Implications in Organic Photovoltaic Charge Generation. *Journal of the American Chemical Society* **2011,** *133* (31), 12106-12114.
13. Murthy, D. H. K.; Melianas, A.; Tang, Z.; Juska, G.; Arlauskas, K.; Zhang, F. L.; Siebbeles, L. D. A.; Inganas, O.; Savenije, T. J., Origin of Reduced Bimolecular Recombination in Blends of Conjugated Polymers and Fullerenes. *Advanced Functional Materials* **2013,** *23* (34), 4262-4268.
14. Wojcik, M.; Tachiya, M., Accuracies of the empirical theories of the escape probability based on Eigen model and Braun model compared with the exact extension of Onsager theory. *The Journal of Chemical Physics* **2009,** *130* (10), -.
15. McMahon, D. P.; Cheung, D. L.; Troisi, A., Why Holes and Electrons Separate So Well in Polymer/Fullerene Photovoltaic Cells. *Journal of Physical Chemistry Letters* **2011,** *2* (21), 2737-2741.